J Mater Sci (2007) 42:3944–3950
DOI 10.1007/s10853-006-1478-5

Microconfigured piezoelectric artificial materials for hydrophones

Aaron T. Crumm · John W. Halloran · Emilio C. N. Silva · Francisco Montero de Espinosa

Received: 16 November 2005 / Accepted: 21 December 2006 / Published online: 11 May 2007
© Springer Science+Business Media, LLC 2007

Abstract Piezoelectric PZT–air composites with a complex design optimized for hydrophones were fabricated as arrays of hundreds of 60 μ units using a microfabrication technique involving coextrusion of mixtures of thermoplastic with PZT powder or carbon powder. The measured piezoelectric coefficient was 300 pC/N with a figure of merit of 18 pm^2/N, in excellent agreement with the predicted properties.

Introduction

The general concept of creating designed structures with specific properties is familiar for large objects, such as vehicles or buildings. Usually designers heuristically optimize for such goals as maximum strength for minimum material. More recently, optimal design techniques have used computational optimal design methods and have addressed other properties. An example is the topology optimization and homogenization algorithm pioneered by Bendsøe and Kikuchi in 1988 [1]. The technique is used to design the fine-scale structure for composite materials with pre-determined (prescribed) or improved properties not available in common materials. Such a fine-scale composite structure can be considered an ''Artificial Material'' (AM). This paper addresses piezoelectric artificial materials optimized for sensitivity as hydrophones, from a microconfigured composite design of lead zirconate titanate (PZT) and air.

The topology optimization and homogenization method used to design piezoelectric composites with elastic and piezoelectric coefficients optimized for transducer are presented in detail elsewhere [2–5]. Very briefly, the design algorithm considers a small unit that, in this case, consists of voxels of solid piezoelectric material and voids. The properties are computed from the staring arrangement of voxels, and compared to the target properties. The algorithm progresses through a series of iterations that refines an arrangement of voxels (three dimensional pixels) towards a user defined property target. The ultimate goal of the process is to develop a repeat unit of solid and void voxels, which achieves agreement with the initial property target. Finite Element Analysis (FEA) is done on the unit cell to calculate a set of homogenized properties that describe the interaction of its boundaries with an infinite number of identical neighbors. Proper homogenization reduces the computing power required to reach a solution so that is becomes practical to perform many design iterations. The computer assembles an array of many unit cells and the calculated macro-properties are compared against the user defined property goal and any other constraints imposed on the problem (stiffness, volume fraction, Poisson ratio [6], piezoelectric response, coefficient of thermal expansion [7], etc.). If the solution is not converged, the algorithm enters a topology optimization subroutine where

A. T. Crumm · J. W. Halloran (✉)
Department of Materials Science and Engineering, University of Michigan, 3062 Dow Building, Ann Arbor, MI 48109-2136, USA
e-mail: john_halloran@engin.umich.edu

E. C. N. Silva
Department of Mechatronics and Mechanical Systems Engineering, Escola Politécnica, University of São Paulo, Sao Paulo, Brazil

F. Montero de Espinosa
Instituto de Acústica, Consejo Superior de Investigationes Cientificas, Madrid, Spain

voxels of solid and void are added and deleted from the unit cell according to a set of sensitivity analysis results. The revised unit cell is used in the subsequent FEA-homogenization iteration. The process continues until the results converge on a local optimum. The optimally designed unit cell is the basis for a PZT–air composite transducers produced as an array of many of the unit cells. This paper presents the fabrication and hydrophone properties for two-dimensional piezoelectric transducers with enhanced hydrophone responses. The fabrication was accomplished assembling a single unit cell, followed by repeated extrusion to produce an array of many microscopic unit cells, using the technique of microfabrication by coextrusion (MFCX) [8].

Piezocomposites and hydrophones

The relationship between the induced polarization and the applied stress [9] is expressed by the third-rank tensor of piezoelectric coefficients, d_{ijk} units of picocoloumbs per Newton (pC/N). For the case of a hydrostatic stress state, we consider the hydrostatic piezoelectric response d_h of material is the sum of the piezoelectric terms from all three directions simultaneously, Eq. 1.

$$d_h = d_{33} + d_{13} + d_{23} \tag{1}$$

The net hydrostatic response of a block of piezoelectric PZT is roughly negated [10, 11] by the equal but opposite contributions from d_{33} and (d_{13} + d_{23}). Thus solid blocks or PZT have a relatively poor d_h values. A hydrophone transducer is employed as a sensor, and its sensitivity is determined by the voltage produced in response to a hydrostatic pressure wave. The hydrostatic voltage coefficient, g_h, relates the measured voltage to an applied hydrostatic stress. The g_h and d_h terms are related by the relative permittivity of the material K according to Eq. 2 (ε_o is the permittivity of free space). A useful figure of merit for a hydrophone transducer is the product of the hydrostatic piezoelectric response d_h and the hydrostatic voltage coefficient g_h. Equation 3 expresses the hydrophone figure of merit, $d_h g_h$, has units of $m^2\ N^{-1}$.The hydrophone figure of merit can be increased by designing a transducer that either increases the hydrostatic piezoelectric response, decreases the permittivity or some combination of both.

$$g_h = \frac{d_h}{\varepsilon_o K} \tag{2}$$

$$d_h g_h = \frac{d_h^2}{\varepsilon_o K} \tag{3}$$

Research efforts into improving hydrophone transducer performance can be classified as either modifications that seek to enhance the materials properties of the piezoelectric ceramic, or designs that improve performance by creating piezocomposites. Efforts to enhance the material properties of electroactive ceramics have included the formulation of new ferroelectric compositions, the use of dopants to modify the dielectric, piezoelectric, and coupling coefficients of electroactive ceramics, and most recently the growth of single crystals [12–16]. While these efforts have succeeded in delivering materials with improved d_h values, maximum benefit is gained by increasing the d_h value while simultaneously decreasing the transducer permittivity. This has been accomplished through the careful design of piezocomposites [17], combinations of piezoelectrics with non-piezoelectric materials. Highly sensitive piezocomposites exist ultrasonic and hydrophone transducers.

One of the most common piezocomposite architectures is the 1-3 piezocomposite invented by Klicker et al. [18]. The 1-3 designation refers to the number of dimensions in which the ceramic and polymer phases are continuously connected [19]. The manner in which the active and inactive phases of a composite are interconnected determines the distribution of electric field and distribution of stress, and therefore the performance of the composite. The hydrostatic response of 1-3 composites is decreased by the high Poisson' ratio of the encapsulating polymer [20]. The internal stress created during mechanical excitation opposes the applied stress and hence reduce the net stress amplification on the ceramic phase [21]. Modifications to the 1-3 design have been proposed minimize this effect [22–24]. Several other piezocomposite designs exist that exploit alternate connectivity, such as 0-3 composites [25] or composites with three-dimensional connectivity [26]. Radially poled hollow spheres [27] composites exhibit pressure independent d_h values in excess of 1,000 pC/N. Piezoceramic–air composite hydrophones with arrays of ordered flat voids have been fabricated by printing fugitive ink on tape cast sheets of PZT [28, 29]. More recently 2-2 piezocomposite made from alternately stacked sheets of piezoceramic and soft polymer and operated in transverse mode [30]. When combined with rigid end caps, the 2-2 piezocomposite yields a $d_h g_h$ value of 30 pm^2/N. The Moonie is a ceramic–metal composite flextensional actuators. Moonies used as hydrophones are reported [30] to have $d_h g_h$ values as high as 50 pm^2/N.

Topology optimized piezocomposites

Figure 1 shows Design 1, which has repeat unit comprised of a 20 × 20 pixelated grid of PZT (black) and air (white)

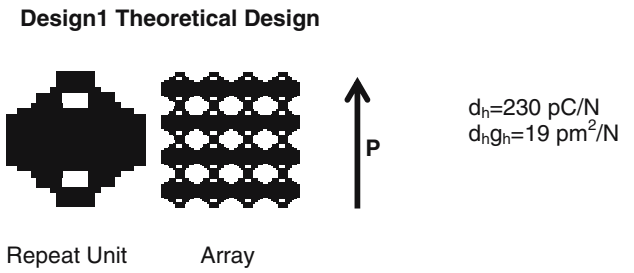

Fig. 1 Theoretical topology optimized PZT–air piezocomposite hydrophone Design 1. A single repeat unit and partial array are illustrated along with the polarization direction and predicted performance values

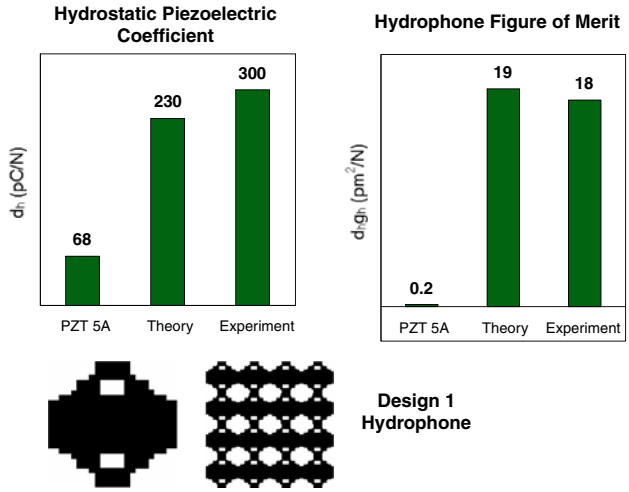

Fig. 3 Design 1 experimental and theoretical values for the hydrostatic piezoelectric response and hydrophone figure of merit. Note the significant improvement of the optimized hydrophone design relative to PZT 5A and the close agreement between the theoretical and experimental results

phases. A partial hydrophone array is included to demonstrate their alignment and connectivity in the final composite. The polarization direction is through the thickness of the piezocomposite as indicated in the figure. The calculated values for the hydrostatic charge coefficient (d_h) and the hydrophone figure of merit ($d_h g_h$) are 230 pC/N and 19 pm^2/N, respectively. These values are compared against several of the best piezocomposite architectures in Figs. 2 and 3.

Design 1 feedrod fabrication and coextrusion

An extrudable compound of powder and thermoplastic was prepared by mixing powder with melted polymer in an electrically heated high intensity shear mixer (Brabender Corp, Model PL2100, USA). The PZT powder (American Piezoelectric PZT856, USA) was surface treated by ball milling for 12 h with ½″ cylindrical zirconia media together with one weight percent stearic acid suspended in isopropyl alcohol. The average particle size, d_{50}, of the PZT powder was measured to be 1.0 μ. The carbon black fugitive powder (Cabot Carbon Black-Black Pearls 120, USA), with a d_{50} value of 75 nm, was used directly from the container. The thermoplastic was an ethylene copolymer based blend as reported previously [31]. The fugitive (at 44 vol% loading) and PZT (at 52.7 vol% loading) were compounded to equivalent apparent viscosity values of 2,300 ± 120 Pa s at an apparent shear rate of 111 ± 4 s^{-1} and stock temperature of 125 ± 1 °C. The PZT and fugitive compounds were extruded into sheets one millimeter thick using a stainless steel extrusion die.

Extrusion was conducted using a piston extruder, which forces as solid block of the powder-EEA compound (a feedrod) through a heated die. Since, the flow behavior of the PZT-EEA compound and the carbon black-EEA compound were adjusted to be very similar, these two compounds can be extruded together, or coextruded. Thus a feedrod having the design of PZT-carbon black unit cell could be reduced in size without distorting the cross section. These extruded sections could be re-assembled and coextruded repeatedly.

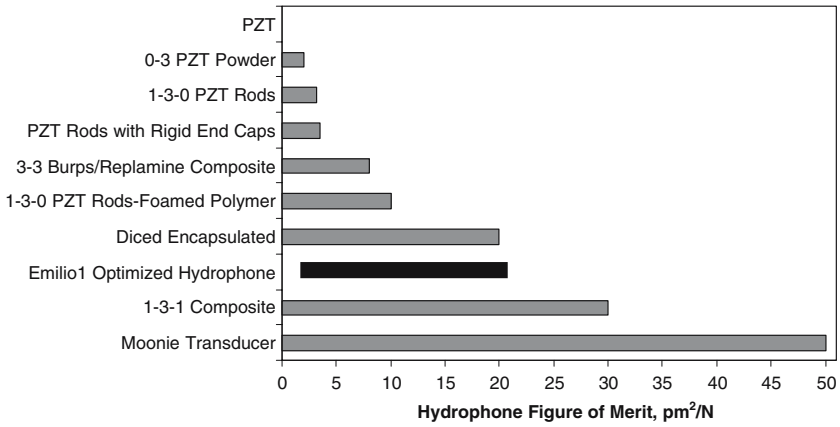

Fig. 2 Comparison of $d_h g_h$ values for various piezocomposites, after Safari [20] with the Optimize Design 1

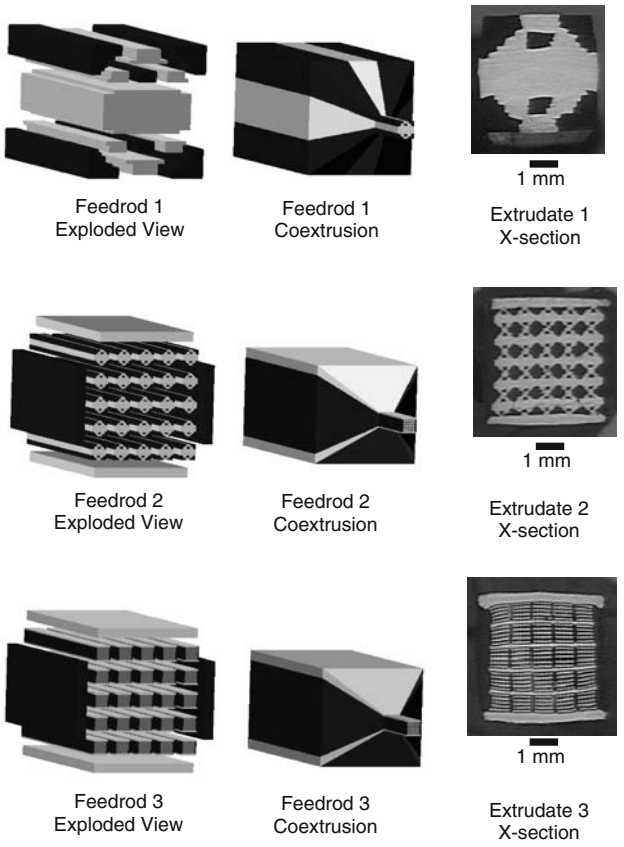

Fig. 4 Design 1 hydrophone fabrication methodology illustrating the first, second, and third coextrusion steps. Optical images of extrudate from each coextrusion step are included to the right

To fabricate the first feedrod, PZT-EEA ceramic and carbon black-EEA fugitive sheets were cut to shape and assembled as shown in Fig. 4 in the design of one unit cell. The assembly was uniaxially pressed at 9 MPa and 160 °C to create a consolidated feedrod containing the piezocomposite repeat unit. The parallelepiped feedrod was extruded through a symmetric 6:1 square reduction at 120 °C and 4 mm/min. The material exiting the extrusion die was reduced in size by a factor of six without distorting the cross sectional structure. The optical image located to the right of the three-dimensional coextrusion illustration depicts the size reduction and shape retention of the coextrusion process.

Lengths of the first extrudate from the first coextrusion pass were bundled together with sheets of ceramic and fugitive compound to create a 25-element array of repeat units. The assembly was uniaxially pressed at 9 MPa and 160 °C to create a second feedrod. The coextrusion process was repeated with the second feedrod. Twenty-five lengths of extrudate from the second extrusion step were cut to equal lengths, bundled together with sheets of ceramic and fugitive compound, uniaxially pressed, and coextruded a third time to create the final green piezocomposite structure. The third extrudate contained 625 repeat units arranged in a continuous two-dimensional array. Cross sectional optical micrographs from each extrusion step are shown along with their respective 3-d illustrations in Fig. 4.

The extra piezoceramic and fugitive materials about the periphery of the second and third feedrods were added to ensure accurate registration between neighboring repeat units. It is important to point out that these additions should not affect the performance.

A portion of third extrudate was sectioned into 1 cm lengths using a sharp blade and cofired in a two-stage process. The parts were laid on a setter bed of PZT + ZrO_2 to avoid contact with the alumina crucible. In the first stage, the thermoplastic binder was removed during a 60 h binder burnout to 700 °C in flowing air. The binder removal heating schedule was devised from thermogravimetric analysis of the extrusion compounds, Fig. 5. Binder burnout and fugitive removal was accomplished by thermally processing in a flowing air atmosphere according to the following schedule; 90 °C/h to 170 °C with a 0.1 h hold, 5 °C/hr to 225 °C with a 1.0 h hold, 4 °C/h to 265 °C with a 1.0 h hold, 8 °C/h to 325 °C with a 1.0 h hold, 20 °C/h to 400 °C with a 0.5 h hold, and 60°C/h to 650 °C with a 0.1 h hold. Once binder burnout was completed, the parts were sealed in an alumina crucible containing PZT + ZrO_2 setter bed powder. The parts were sintered by heating at 3 °C/min to 1,300 °C and holding for 2.0 h in air.

A simple slab-shaped test coupon, with identical processing and sintering, was fabricated to provide specimens to accurately determine the density and properties of the

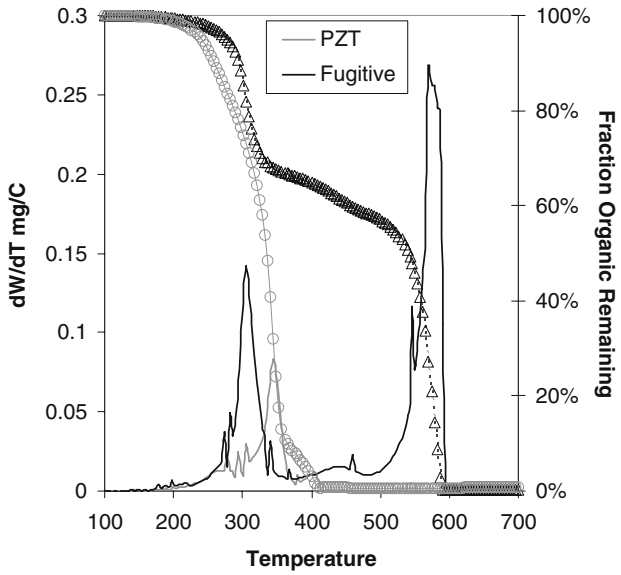

Fig. 5 Thermogravimetric analysis of the binder burnout and fugitive powder removal processes

coextruded PZT. The density of the PZT was measured to be 7.5 g/cm^3 using the standard Archimedes technique, which is 97.5% of the theoretical density reported by the manufacturer. Figure 6 shows the polished and etched microstructure. The average grain size by the linear intercept method is 4.6 μ and a point count suggests 2% residual porosity. A small fraction of a phase in darker contrast was rich in NiO and MgO.

The piezoelectric properties of test coupons fabricated from sheets of PZT coextrusion compound, after poling at 2 kV/mm and 150 °C followed by 24 h of aging, were d_{33} = 100 pC/N using the Berlincourt d_{33} meter and the impedance method, (HP impedance analyzer, model HP4194A, USA coupled with TSI Software, PRAP software, Canada). This agrees with the manufacturer's predicted value of 70 pC/N. According, the material formed by the MFCX technique can be considered a well-formed PZT ceramic with respectable microstructure, a minimal amount of secondary phases, and piezoelectric properties that match reported values.

The final sintered structure for Design 1 is pictured in Fig. 7 as an as-fired SEM micrograph of the piezocomposite cross section. The SEM image illustrates the feature retention achieved during extrusion, the theoretical design is inset into the SEM image for comparison. We consider this quite good reproduction of the complex repeat unit, considering that it has been reduced by a factor of 216 times through three extrusion stages. The final perforated hydrophone (micro-configured voids left behind by the removal of the fugitive material) is made up of an arrangement of twenty-five 5×5 arrays of repeat units measuring 80 μ across with 25 μ features and a net cross sectional density of 3,000 repeat units per centimeter squared. A comparison between the fine features of the part and the measured grain size implies portions of the fabricated part are only 2–3 ceramic grains across.

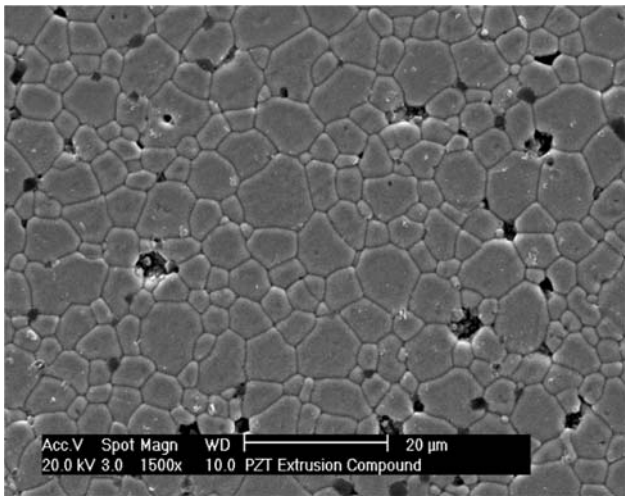

Fig. 6 Polished and thermally etched PZT coextrusion material after sintering, average grain size of 4.6 μ and 98% theoretical density

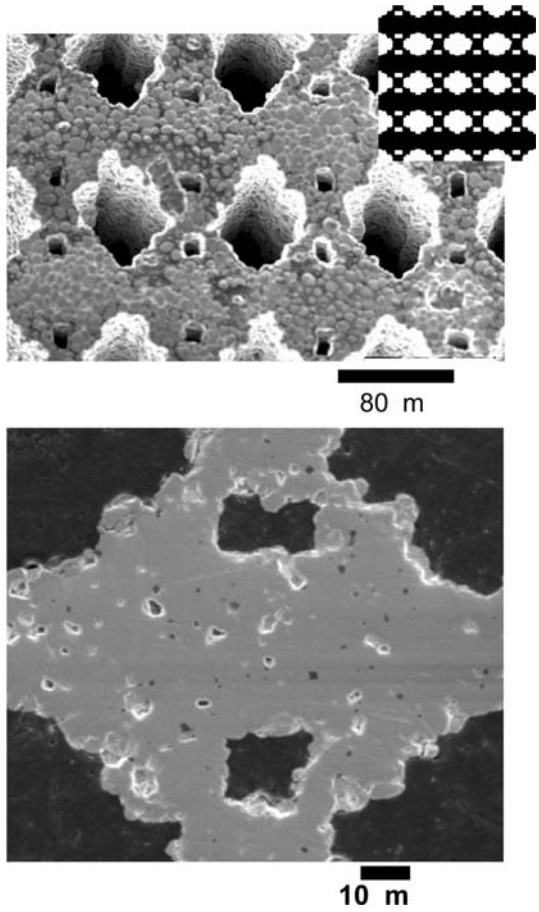

Fig. 7 As fired SEM and polished micrographs of the MFCX Design 1 hydrophone. The ceramic transducer exhibits open channels, 80 μ repeat units, 25 μ feature sizes, and 3,000 repeat units per square centimeter

Design 1 hydrophone fabrication results and testing

Samples of the sintered Design 1, approximately 4 mm cubes in size (with 625 repeat units), were sent to Dr. Francisco Montera de Espinosa at the Instituto de Acoustica, in Madrid, who kindly performed the hydrophone property evaluation. The samples were poled in oil a field of 1.5–2 kV/mm at 140 °C (the Curie temperature is 150 °C for this PZT). Figure 2 shows the piezoelectric charge coefficient and figure of merit of the PZT–air Artificial Material. Note that the hydrostatic charge coefficient of the Optimally Designed PZT hydrophone, with its micro-configured voids, is 300 ± 50 pC/N. This value 4.4 times greater than solid PZT. More exciting is the agreement between experiment (250–350 pC/N for repeated samples) and predicted value for this design (260 pC/N).

We consider this an outstanding agreement, for our relatively crude fabrication. The figure of merit for these optimally designed PZT–air hydrophones, also shown in Fig. 2, is measured to be 18 pm^2/N, virtually identical to Design 1 prediction of 19 pm^2/N, and a remarkable 9,500% improvement of over solid PZT at only 0.2 pm^2/N.

Second generation topology optimized designs

A second generation designs were attempted. These demand extremely fine features (~10 μ) and tighter. The fabrication and sintering conditions were similar. They differ in that the compounding conditions were improved to allow a solids loading of 56 vol% for the PZT, which was rheologically matched to carbon black fugitive at 43 vol%. In this case the final samples were arrangements of forty-nine 7 by 7 arrays of repeat units, each measuring 60 μ across with about 10 μ features and a net cross sectional density of 15,000/cm^2.

Figure 8 shows the ''square geometry,'' a heuristically determined design intended to allow the direct performance comparisons with topology optimized designs. Simulation of this square design predicts a $d_h g_h$ around 6 pm^2/N. These square channels were fabricated with walls about 10 μ wide and 60 μ repeat units. Optimal Design 2 appears in Fig. 9. This was predicted to have extremely large $d_h g_h$ 32.1 pm^2/N. It consists of very slender vertical columns with slots where it connects to the horizontal rectangles. In this case the 10 μ wide vertical columns are only 1–4 grains wide, so this is at the limit of resolution for a sintered ceramic with this grain size. Figure 10 shows the structure of Design 3, which was predicted to have a figure of merit of 16.6 pm^2/N. The repeat unit for this design was quite complicated, with sigma-shaped columns. These could not be reproduced well.

Property measurements could not be made because the samples of Designs 2 and 3 physically fractured during poling at 140 °C (T_{curie} = 150 °C) and ~1.5–2.0 kV/mm.

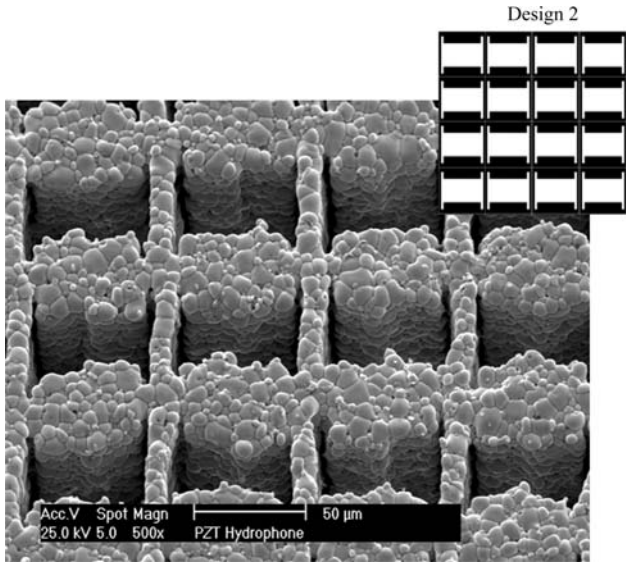

Fig. 9 Design 2 hydrophone fabrication results. The PZT–air piezocomposite is composed of empty square channels, 60 μ repeat units, large aspect ratio 10 μ features, and 15,000 repeat units per centimeter squared

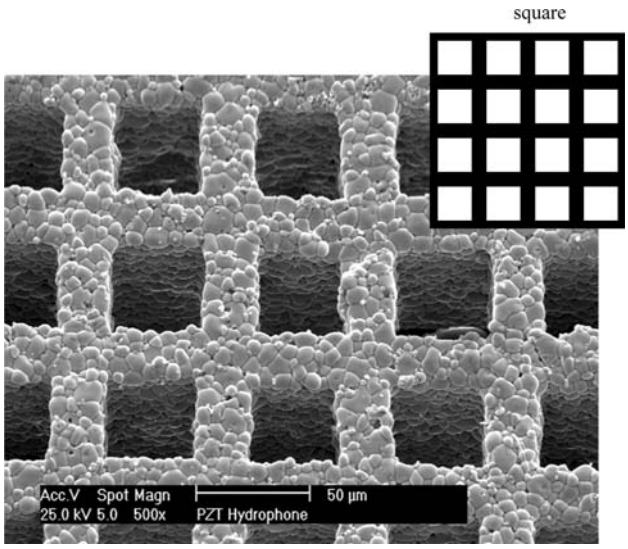

Fig. 8 Square hydrophone fabrication results. The PZT–air piezocomposite is composed of empty square channels, 60 μ repeat units, large aspect ratio 25 μ features, and 15,000 repeat units per centimeter squared

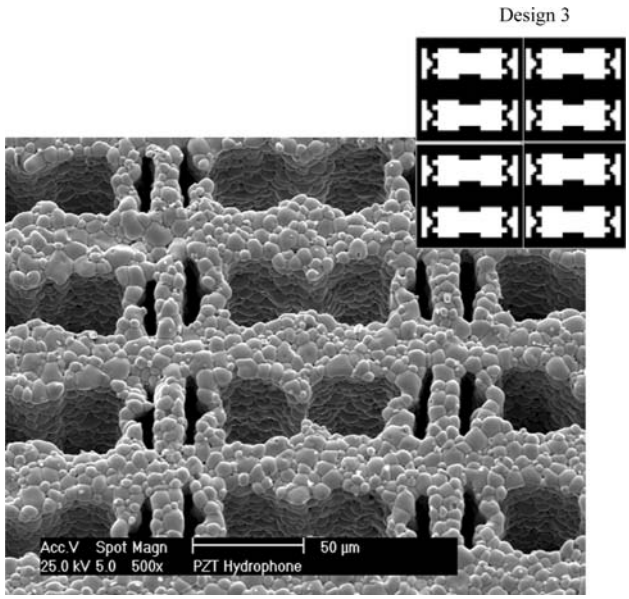

Fig. 10 Design 3 hydrophone fabrication results. The PZT–air piezocomposite is composed of empty square channels, 60 μ repeat units, large aspect ratio ~5 μ features, and 15,000 repeat units per centimeter squared

During the poling process, the hydrophone is mechanically unconstrained, therefore the stresses required to propagate a crack through the samples must be generated internally. We suggest that the mechanism for failure is microcracking imposed by poling stresses. A similar phenomenon was reported by Kahn, Dazell, and Kovel, who suggested cracking of their PZT–air composites from highly localized poling stresses. In our case, it appears that poling stresses aggravated pre-existing processing flaws, which were found in the failed samples returned from Madrid. These flaws were parallel to the extrusion direction, apparently from contamination during green forming. We suggest that fracture during poling was due to synergistic effect involving flaws present in the material, grain size equivalent to feature size effects, stress concentrators resulting from the sharp cornered design, and polarization strains/microcracking effects.

Conclusions

Piezoelectric ceramics can be obtained from PZT using microfabrication by coextrusion to achieve a microstructure and piezoelectric coefficient comparable to conventionally processed PZT ceramic. With the shape capability of this process, it is possible to fabricate piezoelectric hydrophones created by the technique of Optimal Design by the Homogenization Method. A PZT–air composite based on a two-dimensional Optimal Design was predicted to have a hydrostatic piezoelectric coeffient of 230 pC/N and a hydrophone figure of merit of 19 pm^2/N was realized as an array of 625 repeat units, each 80 μ across. The measured piezoelectric coefficient was 300 pC/N with a figure of merit of 18 pm^2/N, in excellent agreement with prediction. This confirms that such designed materials can be accurately designed and practically realized.

Acknowledgement The authors acknowledge the support of the National Science Foundation under DMR 9972620.

Reference

1. Bendsøe MP, Kikuchi N (1988) Comput Methods Appl Mech Eng 71:197
2. Silva ECN (1998) Design of piezocomposite materials and piezoelectric transducers using topology optimization. Ph.D. Thesis, University of Michigan, Department of Mechanical Engineering and Applied Mechanics
3. Silva ECN, Fonseca JSO, Kikuchi N (1998) Comput Method Appl Mech Eng 159:49
4. Silva ECN, Fonseca JSO, Kikuchi N (1997) Comput Mech 19(5):397
5. Sigmund O, Torquato S, Aksay IA (1998) J Mater Res 13(4):1038
6. Crumm AT, Halloran JW (2006) J Mater Sci (JMSC3330 in press)
7. Qi J, Halloran JW (2004) J Mater Sci 39(13):4113
8. van Hoy C, Barda A, Griffith ML, Halloran JW (1998) J Am Ceram Soc 81(1):152
9. Lovett D (1989) Tensor properties of crystals. Institute of Physics Publishing, Bristol, UK
10. Xu Y (1991) Ferroelectric materials and their applications. North Holland-Elsevier Science, New York
11. Jaffe W, Cooke R, Jaffe H (1971) Piezoelectric ceramics. Academic Press, New York
12. Xu Y (1991) Ferroelectric materials and their applications. North Holland-Elsevier Science, New York
13. Jaffe W, Cooke R, Jaffe H (1971) Piezoelectric ceramics. Academic Press, New York
14. Newnham R, Trolier-Mckinstry S, Giniewicz J (1993) J Mater Educ 15:189
15. Park S, Shrout T (1997) J Appl Phys 82(4):1804
16. Park S, Shrout T (1997) IEEE Transac Ultrasonics Ferroelectr Frequency Control 44(5):1140
17. Safari A, Sa-gong G, Giniewicz J, Newnham R (1986) Proc 21st Univ Conf Ceram Sci 20:445
18. Klicker KA, Biggers JV, Newnham RE (1981) J Am Ceram Soc 64:5
19. Newnham RE, Skinner DP, Cross LE (1978) Mater Res Bull 13:525
20. Safari A (1994) J Phys III France 4:1129
21. Swart PJ, Avellaneda M (1994) Adapt Struct Comp Mater: Anal Appl, ASME 1994, AD-Vol 45/MD-Vol 54:59
22. Haun MJ, Newnham RE (1986) Ferroelectrics 68:123
23. Haun M (1983) Ferroelectrics 49:259
24. Richard C, Eyrand P, Eyrand L, Audigier D, Richard M (1992) IEEE Proceedings of ISAF, pp 235–259
25. Safari A, Lee YH, Halliyal A, Newnham RE (1987) Am Ceram Soc Bull 66:668
26. Skinner DP, Newnham RE, Cross LE (1978) Mater Res Bull 13:599
27. Fernandez JF, Dogan A, Zhang QM, Tressler JF, Newnham RE (1995–1996) Sensors Actuat A: Phys 51(2–3):183
28. Kahn M, Dalzell A, Kovel B (1985) J Am Ceram Soc 68(11):623
29. Kahn M (1987) Adv Ceram Mater 2:836
30. Zhang QM, Chen J, Wang H, Zhao J, Cross LE, Trotter MC (1995) IEEE Transac Ultrasonics Ferroelectr Frequency Control 42(4):774
31. Crumm AT, Halloran JW (1998) J Am Ceram Soc 81(4):1053